Proceedings of the CERN-BINP Workshop for Young Scientists in e^+e^- Colliders, Geneva, Switzerland, 22 – 25 August 2016, edited by V. Brancolini ans L. Linssen, CERN Proceedings, Vol. 1/2017, CERN-Proceedings-2017-001 (CERN, Geneva, 2017)

Radiation Hardness Study of CsI(Tl) Crystals for the Belle II Calorimeter

D.V. Matvienko, E.V. Sedov, B.A. Shwartz and A.S. Kuzmin
Budker Institute of Nuclear Physics, SB RAS
and Novosibirsk State University, Novosibirsk, Russia

Abstract
The Belle II calorimeter consists of CsI(Tl) scintillation crystals which have been used at the Belle experiment. A radiation hardness study of typical Belle crystals is performed and it is found that light output reductions are acceptable for the Belle II experiment where the absorption dose can reach 10 krad during the detector operation. CsI(Tl) crystals have high stability and low maintenance cost and are considered a possible option for the calorimeter of the future Super-Charm-Tau Factory (SCT) in Novosibirsk. The study also demonstrates sufficiently high radiation hardness of CsI(Tl) crystals for SCT conditions.

Keywords
Belle II calorimeter; CsI(Tl) crystals; radiation hardness; light output.

1 Introduction

The Belle detector [1] operated at the KEKB factory [2] from 1999 until 2010 was a universal magnetic detector including several sub-detectors and had excellent performance. The electromagnetic calorimeter (ECL) of the Belle detector contained 8736 CsI(Tl) scintillation crystals. Each crystal has a truncated pyramid shape of an average size about 6×6 cm^2 in cross section and 30 cm ($16.1X_0$) in length. The Belle calorimeter based on these crystals demonstrated high quality and performance. Additionally, it had multiple functions.

- The ECL allowed to detect photons in a wide range of energies (from a few MeV to a few GeV) with excellent resolution. The energy resolution achieved at 1 GeV was 1.8% and about 4% at 100 MeV.
- The ECL provided the determination of photon space coordinates. The space resolution was about $5\ \text{mm}/\sqrt{E(\text{GeV})}$.
- The Belle calorimeter also served for the separation of electrons and hadrons.
- Information from the ECL was used for the formation of a neutral trigger signal.
- The ECL provided the luminosity measurement independent from the data acquisition system.

The absorbed dose collected by the crystals during the operation of the Belle experiment is shown in Fig. 1 (see Ref. [3]). The measured integrated dose for the luminosity of 1000 fb^{-1} is about 100 rad for the barrel crystals and 400 rad for the highest-dose endcap crystals. The light output degradation corresponding to the integrated absorbed dose and shown in Fig. 2 is about 7% in the barrel and up to 13% in the endcap parts of the ECL. The results shown in Figs. 1, 2 are in good agreement with previous measurements of the radiation hardness for a large set (55 samples) of the Belle typical crystals [4]. This study has been performed for a distributed absorbed dose up to 3700 rad. However the expected dose for the Belle II endcap crystals is up to 10 krad after 10 years of the Belle II experiment operation. It has been decided to keep all the CsI(Tl) crystals in the Belle II calorimeter, at least at the first stage of the experiment [3]. Thus, the Belle II conditions require an additional measurement of the radiation hardness for the CsI(Tl) crystals. This problem is discussed in Ref. [5]. For our study four crystals produced for the Belle calorimeter but rejected due to their geometry specifications or small mechanical defects have been

https://doi.org/10.23727/CERN-Proceedings-2017-001.55

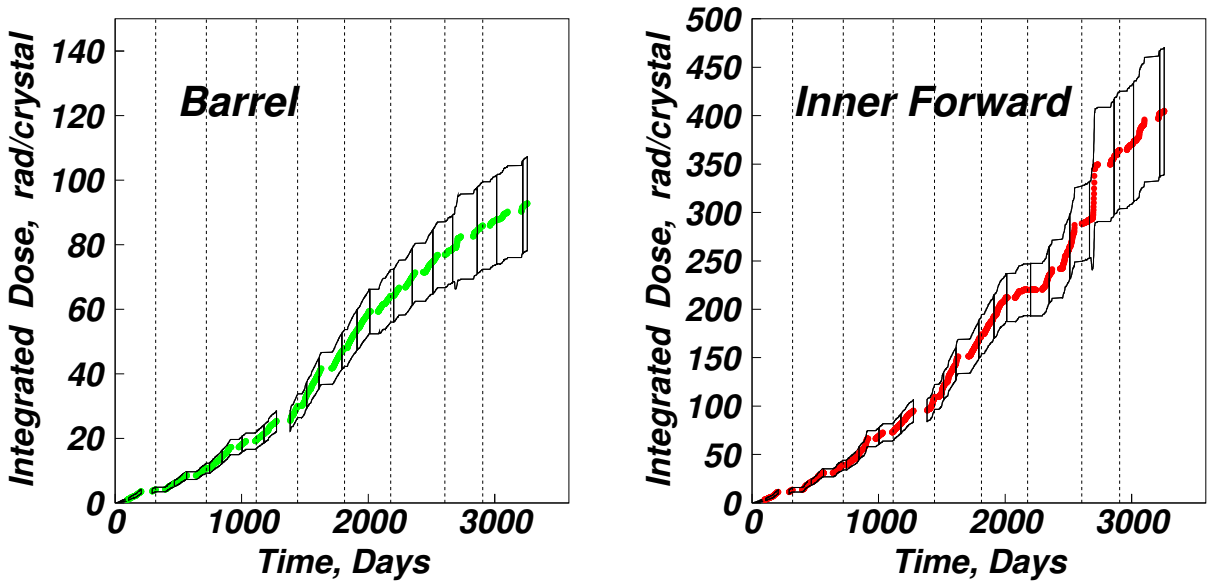

Fig. 1: Integrated absorbed dose collected by the Belle calorimeter based on CsI(Tl) crystals

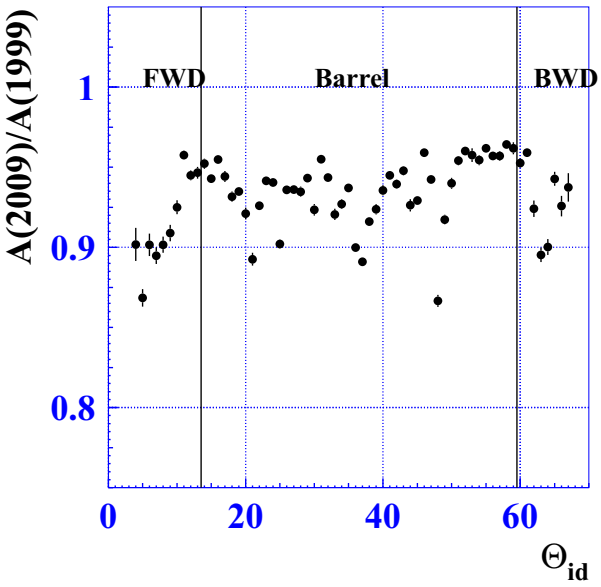

Fig. 2: Light output loss after 10 years of the Belle experiment

selected. Their scintillation properties met Belle requirements. These crystals have shapes of truncated pyramids with slightly different sizes and have been used in a previous study [4] which was held in 2003. Thus, their characteristics are known from this previous radiation hardness study. The measured light output degradation for the studied crystals is shown in Fig. 3. Prior to previous measurements all these crystals were polished, wrapped in 200 μm porous teflon and covered with a 20 μm thick aluminized mylar film. These wrappers are kept in the study.

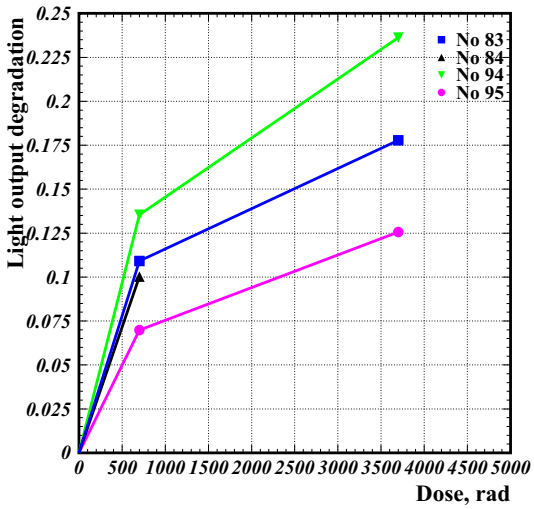

Fig. 3: Light output degradation for the selected crystals 83, 84, 94 and 95 measured in Ref. [4]

2 Crystal irradiation

The studied samples are irradiated with the industrial electron accelerator ELV-6 [6] at Budker Insitute of Nuclear Physics in Novosibirsk. The ELV-6 accelerator provides a continuous electron beam with the energy of 1.4 MeV and a beam current up to 100 mA. The specific features of the ELV-type accelerators are the simplicity of design, convenience and ease in control and also reliability in operation. The scheme of the irradiation setup is shown in Fig. 4. The electron beam hits the converter in which bremsstrahlung

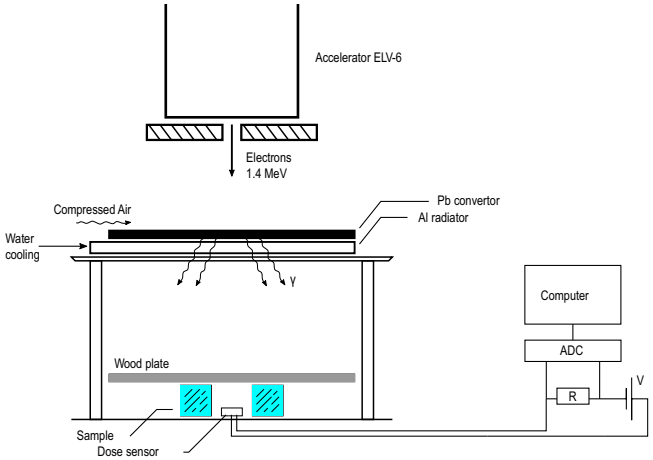

Fig. 4: The setup for irradiation of the crystals with the ELV-6 accelerator

photons are created due to the electron scattering in the converter material. Two different types of converters are used: lead and tantalum. The lead converter containing a 3 mm lead plate and cooled by a water radiator and air flux is used with absorbed doses less than 7 krad. For higher doses the power absorbed in the converter can melt the lead plate. In this case the tantalum converter is used consisting of 0.5 mm of Ta, 2 mm of water and 2 mm of stainless steel. The photons from these converters have a wide energy spectrum with an average value around 0.6 MeV and uniformly irradiate the crystals over an area which is the horizontal surface at about 1m distance below the converter. The wood plate over the crystals is used to suppress the electrons scattered in air.

The average bremsstrahlung photon interaction length in CsI material is about 3 cm. Since the transverse size of the irradiated crystals is about 6 cm, the absorbed dose in the upper side of the crystal is a few times higher than at the bottom one. To compensate this nonuniformity, each sample is irradiated with equal doses from opposite sides.

To control the dose absorbed in the crystals during the irradiation two special designed dose sensors are placed together with the crystals. The dose sensor shown in Fig. 5 consists of a CsI(Tl) crystal with the dimensions $1 \times 2 \times 2$ cm^3 coupled with an optical contact with silicon-based photodiode (PIN diode) Hamamatsu S2744-08 which has an active area of 1×2 cm^2. One more photodiode identical with

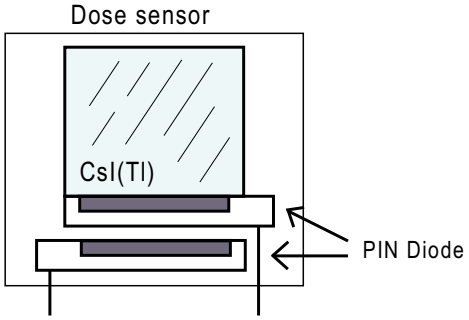

Fig. 5: The dose sensor for the dose rate measurement during the irradiation

the previous one is placed without light connection with the crystal. The second photodiode is needed to control the dark current during irradiation. Currents from two photodiodes are recorded each 100 ms using control resistances and an ADC L-CARD E14-440 connected to a PC. The difference between these currents is taken as the signal current I.

The dose rate $dD/dt = kI$ absorbed in the sensor is proportional to the current I and can be calculated from the average energy deposition per photon $\bar{E}$, the counting rate ν and the crystal mass M:

$$\frac{dD}{dt} = \frac{\bar{E}\nu}{M}. \tag{1}$$

Thus, to calibrate the dose sensor, the coefficient $k = \bar{E}\nu/M/I$ has to be determined.

3 Dose sensor calibration

To determine k, two radioactive ^{137}Cs sources with intensities $\mathcal{J} \sim 10^5$ Bq and $\mathcal{J} \sim 10^8$ Bq are used. Two sources are necessary because the current I cannot be measured with a lower intensity source and the source with higher intensity leads to a significant pile-up effect. Thus, $\bar{E}$ is determined from the spectrum of the lower intensity source shown in Fig. 6. The measured energy threshold is about 100 keV. To take into account the spectrum region below this threshold, a constant approximation is used. Another problem is measuring the counting rate $\nu_{\text{high}}(0)$ for the higher intensity source with null distance from the dose sensor surface. The counting rate $\nu_{\text{low}}(0)$ for the source with $\mathcal{J} \sim 10^5$ is well measured. To calculate $\nu_{\text{high}}(0)$, the relation

$$\nu_{\text{high}}(0) = \frac{\nu_{\text{high}}(r)}{\nu_{\text{low}}(r)}\nu_{\text{low}}(0) \tag{2}$$

is used, where the counting rates $\nu_{\text{high}}(r)$ and $\nu_{\text{low}}(r)$ are measured for a finite distance r perpendicular to the sensor surface when the pile-up effect is not significant. The ratio $\nu_{\text{high}}(r)/\nu_{\text{low}}(r)$ is permanent with good accuracy for control distances r.

The coefficient k measured by this method has an uncertainty of about 15%. The main effect is due to the current measurement I.

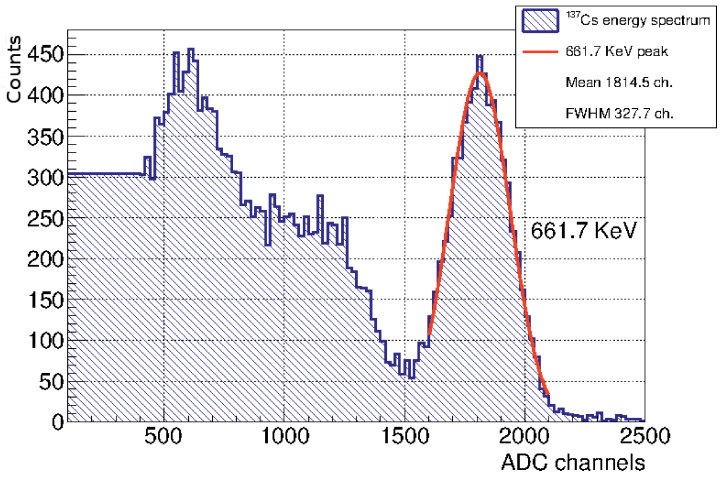

Fig. 6: The spectrum from the ^{137}Cs radioactive source with constant approximation to the region below the threshold.

4 Light output measurements

To measure the scintillation properties of the crystals the testbench shown in Fig. 7 is used. The crystal under study is placed on the input window of the photomultiplier (PMT) Hamamatsu R1847S without optical contact. The PMT R1847S has a bialkali photocathode and a ten dynode system of electron multipliers with a typical gain of the order of 10^7. The radioactive source of ^{137}Cs placed in the lead

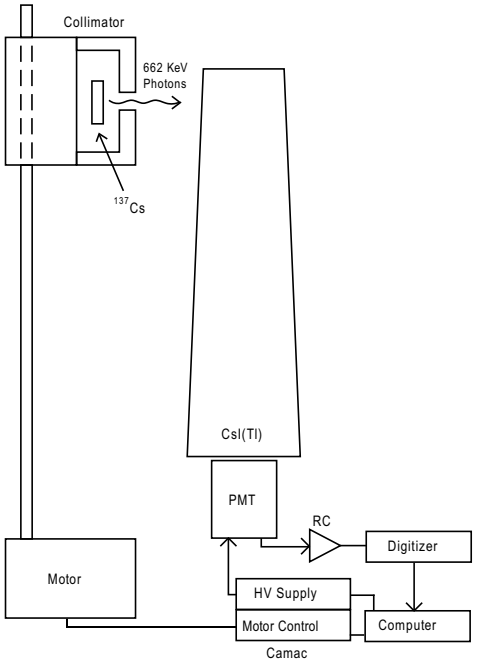

Fig. 7: Testbench for light output measurement

collimator, which can move along the crystal axis and irradiates the crystal with 662 keV photons. The measurements are carried out in nine positions with a step size of 30 mm. The PMT signal after shaping (based on an RC-circuit with the time constant $\tau = 75$ ns) is digitized continuously at a frequency of

250 MHz by a 12 bit multifunctional desktop waveform digitizer CAEN DT5720A [7]. The digitizer houses USB 2.0 which allows data transfers up to 30 MB/s. The digital pulse processing firmware [8] provided with this device allows to record the input signal, integrate the pulse waveform samples within a programmable acquisition gate and save the pulse integral spectrum to a text file. For each spectrum, corresponding to the collimator position, the total absorption position A_i ($i = 1, \ldots, 9$) is determined. The light output of the studied sample is defined relative to the light output for the reference crystal as

$$L_i = \frac{A_i}{A_0}, \tag{3}$$

where A_0 is the photoelectric peak position for the reference crystal, which is a standard CsI(Tl) crystal of 15 mm height and 15 mm diameter packed in the aluminium container.

The average light output is defined as:

$$\bar{L} = \frac{L_1 + \ldots + L_9}{9} \tag{4}$$

and the light output non-uniformity along the crystal axis is defined as

$$\frac{\Delta L}{\bar{L}} = \frac{L_{\max} - L_{\min}}{\bar{L}}, \tag{5}$$

where $L_{\max}$ and $L_{\min}$ are the maximum and minimum values of the light output.

5 Results

Four expositions for selected crystals are performed with the total dose of 30 krad and their light outputs are measured using the above described testbench. Results for the average light output $\bar{L}$ are shown in Fig. 8 (a) for the crystals 83, 84 and in Fig.8 (b) for the crystals 94, 95.

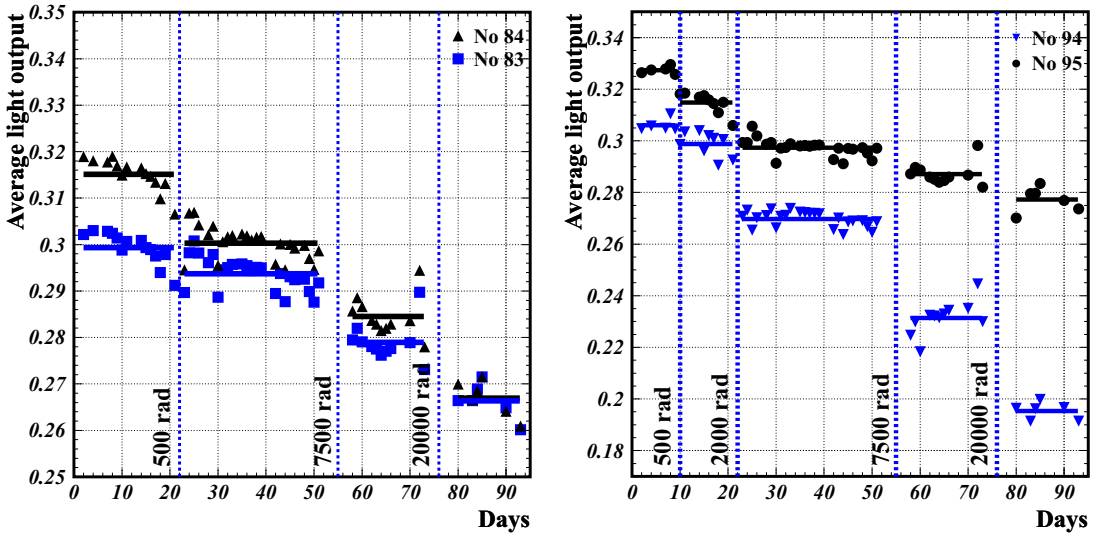

(a) (b)

Fig. 8: Time dependencies of average light output for crystals (a) 83, 84 and (b) 94, 95. Vertical lines show the dose absorbed in the crystals during one exposition.

Different degradations of the average light output are observed. The light output loss for the crystal 94 is not essential after a dose of 500 rad but significantly increases with higher doses (drop of 25% after a dose of 10 krad and 37% after 30 krad). Another effect is observed for the crystals 83, 84 and 95: the light output deterioration is 7 to 10% after a dose of 10 krad and 16 to 18% after 30 krad.

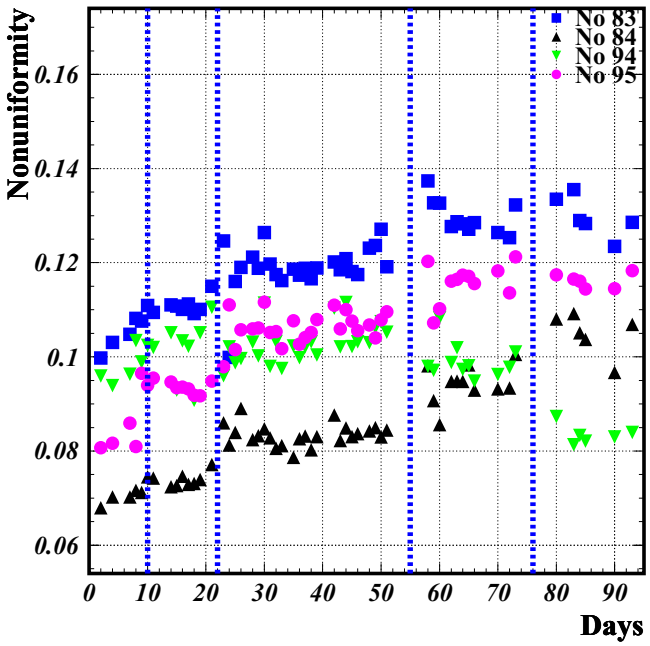

Fig. 9: Time dependence of non-uniformity for the crystals 83, 84, 94 and 95. Vertical lines demonstrate exposition moment.

The measured light-output non-uniformity is shown in Fig. 9. A deterioration of the light output non-uniformity is observed except for the crystal 94, where the opposite tendency takes place after the fourth exposition. The non-uniformity after all expositions is less than 14% for all samples. There are no any stringent requirements on the CsI(Tl) non-uniformity measurements for the Belle II calorimeter because all the crystals used at Belle are kept to be used at Belle II. The non-uniformity for the Belle experiment was required to be less than 9% for all crystals and less than 7% for 90% of total crystals.

It is interesting to combine the results for selected samples with the previous study (see Fig. 3). Since the absolute light output is not measured, the results are normalised to the previous measurements for the crystal 95. This is under the assumption, that the natural recovery of the light output for the crystal 95 is absent and its light output is stable during the period between the studies. The average light output in dependence of the absorbed dose for studied crystals is shown in Fig. 10. The dashed lines in Fig. 10 represent the previous study and the solid lines show the new results. The last values of the previous study are close to the first points of the new study. Thus, the assumption is valid. Fig. 10 also demonstrates that the light output drops slower after increasing the dose for all samples. Another feature is that the behavior of the curves for the average light output loss obtained from the previous measurements is similar for each studied crystal. For example, the crystal 94 has maximum light output loss in both studies.

The degradation of the light output versus the absorbed dose is shown in Fig. 11. As before, the dashed lines correspond to the previous study [4] and solid lines demonstrate the new measurements. The light output loss is described by similar curves for the crystals 83, 84 and 95. The light output degradation after a total dose of about 35 krad is 30% for the crystals 83, 84, 95 and 50% for the crystal 94. The light output drops significantly after all expositions.

According to the latest simulation of a beam-induced background at SuperKEKB, the radiation dose rate for the most radiation loaded parts of the calorimeter can exceed 600 rad/year. Our estimation of the light output degradation at expected doses is demonstrated in Fig. 11. This degradation results in the deterioration of the energy resolution mostly due to the increasing of energy equivalent of the

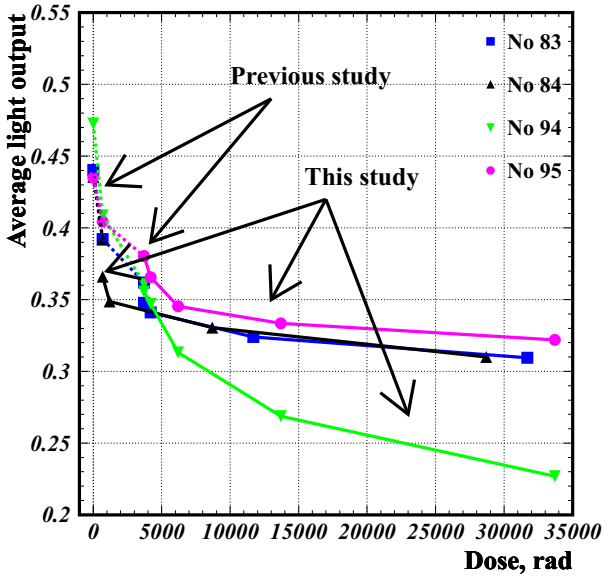

Fig. 10: Average light output in dependence of the total absorbed dose for the crystals 83, 84, 94 and 95 obtained in previous study [4] (dashed lines) and in this study (solid lines).

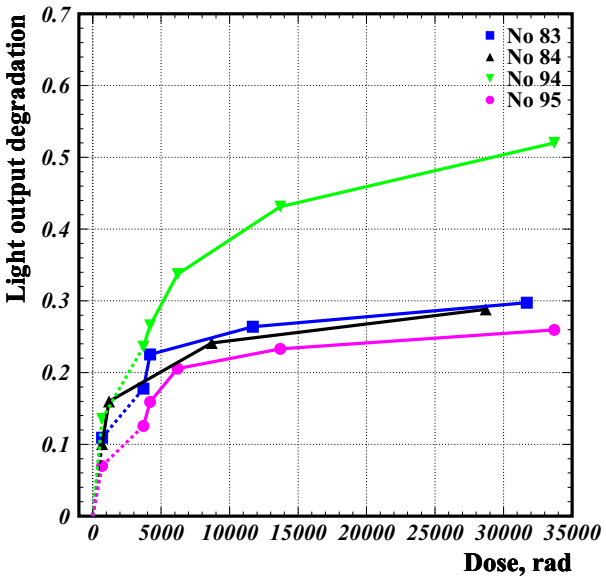

Fig. 11: The distribution of the light output degradation over the total absorbed dose for the crystals 83, 84, 94 and 95 obtained in previous study [4] (dashed lines) and in this study (solid lines).

electronic noise (especially for low energies). The average output signal of the Belle crystals is about 5000 photoelectrons per 1 MeV while the electronic noise level is about 300 keV. The light output loss for the worst tested sample 94 is 40% at the total Belle II expected dose of 10 krad. In such a case, the noise level increases proportionally up to 500 keV. However, the pile up noise with the level of about $2-5$ MeV caused by the soft background photons substantially exceeds the electronic noise (<1 MeV) even for the crystals with relatively low radiation hardness like the crystal 94 [9]. Therefore, the radiation damage of the CsI(Tl) crystals is not the serious problem for the Belle II calorimeter.

6 CsI(Tl) crystals for the calorimeter of the Super Charm-Tau Factory

The future detector of the Super Charm-Tau (SCT) Factory in Novosibirsk should include an electromagnetic calorimeter. Since most of the photons produced in the conditions of this experiment have energies of the order of 100 MeV, the calorimeter needs good resolution for these energies. The Belle calorimeter based on the CsI(Tl) scintillation crystals had excellent performance for the photons in the range of energies. Thus, CsI(Tl) crystals could be considered as possible option for a future SCT calorimeter. These crystals have high light output (5×10^4 photons per MeV) and an emission spectrum with a maximum of about 550 nm matching with the high sensitivity region of the silicon photodiodes. Since the designed SCT luminosity is expected to be 1×10^{35} cm^{-2}s^{-1}, the integrated absorbed dose can reach 1 krad after 5 years of detector operation. This study together with the studies in Refs. [4, 5] demonstrates sufficient radiation hardness of CsI(Tl) crystals for the conditions of e^+e^- colliders including the SCT factory. One more advantage of CsI(Tl) crystals is their low maintenance cost. They are approximately two times cheaper than pure CsI crystals. It is also worth noting that the scientific group from Budker Institute of Nuclear Physics in Novosibirsk has considerable experience of working with alkali-halide crystals such as CsI(Tl).

7 Conclusion

A radiation hardness study of CsI(Tl) crystals produced for the Belle calorimeter has been performed to investigate their scintillation characteristics in conditions of the Belle II experiment. Selected crystals have been exposed in an earlier study with a total dose of about 3.5 krad. In this study four expositions with the integrated dose of 30 krad have been investigated. The results are consistent with the previous measurements. The light output falls faster for doses less than 1 krad and it has more slower degradation for higher doses. The total degradation is about 30% for the three studied samples and 50% for the worst crystal. The relative behavior of the light output loss obtained in the previous measurements for the studied samples remains the same in the study. Measured light output non-uniformity is less than 14% after a dose of about 35 krad.

In summary, the scintillation properties of the Belle CsI(Tl) crystals are acceptable for the Belle II experiment as well as for a SCT factory conditions.

Acknowledgements

This work has been supported by Russian Science Foundation (project N 14-50-00080).

References

[1] A. Abashian *et al.* (Belle Collaboration), *Nucl. Instrum. Methods Phys. Res. A* **479** (2002) 117. https://doi.org/10.1016/S0168-9002(01)02013-7

[2] S. Kurokawa and E. Kikutani, *Nucl. Instrum. Methods Phys. Res. A* **499** (2003) 1. https://doi.org/10.1016/S0168-9002(02)01771-0

[3] T. Abe *et al.*, Belle II technical design report, arXiv:1011.0352.

[4] D.M. Beylin *et al.*, *Nucl. Instrum. Methods Phys. Res. A* , **541** (2005) 501. https://doi.org/10.1016/j.nima.2004.11.023

[5] S. Longo and J.M. Roney, *J. Instrum.* **11** (2016) P08017. https://doi.org/10.1088/1748-0221/11/08/P08017

[6] S.N. Fadeev *et al.*, *Radiat. Phys. Chem.* **57** (2000) 653.

[7] E-publishing service, DT5720 user manual, www.caen.it/servlet/checkCaenManualFile?Id=10257.

[8] E-publishing service, Digital Pulse Charge Integrator user manual, www.caen.it/servlet/checkCaenManualFile?Id=11275.

[9] V. Aulchenko *et al.*, *J. Phys. Conf. Ser.* **587** (2015) 012045.
https://doi.org/10.1088/1742-6596/587/1/012045